# In-Field Performance Testing of the Fork Detector for Quantitative Spent Fuel Verification*

**I. Gauld[1], J. Hu[1], P. DeBaere[2], S. Vaccaro[2], P. Schwalbach[2], H. Liljenfeldt[3], S. Tobin[4]**

[1] Oak Ridge National Laboratory
P.O. Box 2008, Oak Ridge, TN 37831-6170 USA
E-mail: gauldi@ornl.gov
[2] European Commission, DG Energy, Directorate Nuclear Safeguards
[3] Swedish Nuclear Fuel and Waste Management Company
[4] Los Alamos National Laboratory

**Abstract:**

Expanding spent fuel dry storage activities worldwide are increasing demands on safeguards authorities that perform inspections. The European Atomic Energy Community (EURATOM) and the International Atomic Energy Agency (IAEA) require measurements to verify declarations when spent fuel is transferred to difficult-to-access locations, such as dry storage casks and the repositories planned in Finland and Sweden. EURATOM makes routine use of the Fork detector to obtain gross gamma and total neutron measurements during spent fuel inspections. Data analysis is performed by modules in the integrated Review and Analysis Program (iRAP) software, developed jointly by EURATOM and the IAEA. Under the framework of the US Department of Energy–EURATOM cooperation agreement, a module for automated Fork detector data analysis has been developed by Oak Ridge National Laboratory (ORNL) using the ORIGEN code from the SCALE code system and implemented in iRAP. EURATOM and ORNL recently performed measurements on 30 spent fuel assemblies at the Swedish Central Interim Storage Facility for Spent Nuclear Fuel (Clab), operated by the Swedish Nuclear Fuel and Waste Management Company (SKB). The measured assemblies represent a broad range of fuel characteristics. Neutron count rates for 15 measured pressurized water reactor assemblies are predicted with an average relative standard deviation of 4.6%, and gamma signals are predicted on average within 2.6% of the measurement. The 15 measured boiling water reactor assemblies exhibit slightly larger deviations of 5.2% for the gamma signals and 5.7% for the neutron count rates, compared to measurements. These findings suggest that with improved analysis of the measurement data, existing instruments can provide increased verification of operator declarations of the spent fuel and thereby also provide greater ability to confirm integrity of an assembly. These results support the application of the Fork detector as a fully quantitative spent fuel verification technique.

**Keywords:** Fork detector; iRAP; spent fuel verification; ORIGEN; spent fuel safeguards

## 1. Introduction

Spent fuel safeguards rely primarily on material containment and surveillance with item counting and non-destructive assay (NDA) verification measurements. Such measurements are required for spent fuel assemblies before they are transferred to long-term dry storage, final disposal at a repository or, in general, to other facilities where assemblies are not easily accessible. Verification measurements may also be required to re-establish continuity of knowledge. The instruments currently accepted by

* This manuscript has been authored by UT-Battelle, LLC under Contract No. DE-AC05-00OR22725 with the U.S. Department of Energy. The United States Government retains and the publisher, by accepting the article for publication, acknowledges that the United States Government retains a non-exclusive, paid-up, irrevocable, world-wide license to publish or reproduce the published form of this manuscript, or allow others to do so, for United States Government purposes. The Department of Energy will provide public access to these results of federally sponsored research in accordance with the DOE Public Access Plan (http://energy.gov/downloads/doe-public-access-plan).

the International Atomic Energy Agency (IAEA) for spent fuel measurements are the Fork detector and the Cerenkov Viewing Device (CVD) [1].

Activities related to spent fuel storage and disposal are increasing in Europe and worldwide as spent fuel pools reach their storage capacities and many countries are expanding dry storage operations and some are seeking extended interim storage options. In Europe, the increasing use of dry cask storage has increased the demands on safeguards authorities to perform inspections during cask loading. Measurements are routinely performed using the Fork detector during joint inspections by the IAEA and the European Atomic Energy Community (EURATOM). The Fork instrument relies on passive gross gamma-ray and total neutron counting as a means to indirectly verify the operator declarations of the fuel. The Fork detector has been used for safeguards since the 1980s; the underlying technology has remained largely unchanged over 30 years, owing to its simplicity, durability, transportability, and the fast and relatively low-intrusive nature of the measurements.

To address increasing demands on inspection resources and to improve the efficiency of data collection, EURATOM developed the Remote Acquisition of Data and Review (RADAR) unattended data acquisition software application, which can operate without the presence of an inspector [2]. Data analysis, review, and reporting are performed by the Integrated Review and Analysis Program (iRAP), developed jointly by EURATOM and the IAEA. To enable analysing the Fork measurement data quantitatively and identifying potential discrepancies between operator declarations and measurements, an automated spent fuel data analysis module has been implemented in iRAP. This module is based on the ORIGEN code [3], developed and maintained at the Oak Ridge National Laboratory. Software development, integration, and testing have been done under a collaboration agreement between the US Department of Energy (DOE) and EURATOM. Unlike some research initiatives focusing mainly on new and advanced detector technologies, the current research focuses rather on improving the accuracy and efficiency of the data analysis for a proven technology (the Fork detector), thereby minimizing the impact on existing inspector requirements or facility operations.

Benchmarking and validation of the spent fuel analysis module in iRAP have been performed using measurement data acquired through cask loading campaigns in Europe during joint inspections using both EURATOM and IAEA Fork instruments and electronics. In the past two years, data from more than 15 loading campaigns and more than 200 assemblies have been evaluated [4, 5]. However, cask loading data are inherently limited by low assembly diversity. Frequently, the assemblies have the same or similar enrichments, burnup, and cooling times. Consequently, the limited assembly properties do not provide sufficient challenges to test the analysis capabilities. Additionally, finding patterns or trends within such limited data set has proven to be difficult.

The research presented in this paper includes an analysis of recent Fork measurements performed on assemblies at the Swedish Central Interim Storage Facility for Spent Nuclear Fuel (Clab), in Oskarshamn, Sweden. These assemblies have been selected for measurements under the US DOE Office of Nuclear Nonproliferation and Arms Control's Next Generation Safeguards Initiative Spent Fuel (NGSI-SF) Project, in collaboration with the EURATOM Directorate for Nuclear Safeguards, and the Swedish Nuclear Waste Management Company, Svensk Kärnbränslehantering AB (SKB). The assemblies selected under this experimental program cover a very wide range of spent fuel characteristics that are representative of commercial fuels. Extensive fuel design and detailed operating history data are also available for all assemblies included under this program. Such a diverse data set provides a valuable opportunity to quantify the performance of the Fork detector and data analysis methods. Furthermore, the results discussed in this paper, which are representative of current technology capabilities, can be used to benchmark results obtained with the more advanced instruments and techniques.

## 2. Facility and experimental program

Under the DOE NGSI-SF project, several advanced NDA instruments have been developed for assembly measurements to advance the state-of-the-art in NDA techniques for spent fuel verification [6]. Under the US International Nuclear Safeguards Engagement Program (INSEP) and in the framework of the EURATOM-DOE Technical Cooperation Agreement on nuclear safeguards and security, an Action Sheet has been agreed between SKB, EURATOM, and DOE. Several instruments are being deployed for testing and performance evaluation at the Clab facility in Sweden. Operated by SKB, Clab is the central interim storage facility for all spent nuclear fuel from 12 commercial reactors in Sweden. More than 30,000 spent fuel assemblies are currently stored in the pools at Clab, with plans for a final repository in Forsmark to become operational after 2030.

Within the experimental program, 50 spent fuel assemblies were selected for measurements that span the wide range and diversity of fuels that are intended to go in the Swedish repository. The fuel design and operating characteristics of 25 assemblies from pressurized water reactors (PWRs) and 25 from boiling water reactors (BWRs) are listed in Table 1. The PWR assembly designs include 15×15 and 17×17 lattice types, while the BWR assembly designs include 8×8 (with and without water rods), 10×10 SVEA and 10×10 ATRIUM lattice designs.

The 25 PWR assemblies have an enrichment range from 2.1% to 4.1% and a burnup range from 19.6 to 52.6 GWd/tU. The cooling times span from 4.2 to 29.2 years. The 25 BWR assemblies have enrichments from 1.3% to 4.0%, burnups from 9.1 to 46.4 GWd/tU, and cooling times between 7.2 and 29.2 years.

In addition, several assemblies had complex irradiation histories, where the assembly was unloaded from the reactor for several cycles between its initial loading and final discharge. The irradiation history is indicated approximately in Table 1 by the percent effective full-power days (%EFPD). This parameter represents the percentage of time that a particular assembly is irradiated at full power rate between its initial loading and final discharge. Assemblies with low %EFPD values generally experienced either significant outages (within cycle and/or between cycles) or long periods of low power operation while irradiated in the core. For example, assembly PWR24 was out of core for about 10 years before it was re-loaded in the core, resulting in a low %EFPD of 11%. BWR25 was loaded in the first cycle of the reactor and it experienced long periods of low power operation, resulting in a %EFPD of 31%.

| Assembly Identifier | Assembly Design | Enrichment ($^{235}$U%) | Burnup (GWd/tU) | Cooling time (yr) | Loading date (month/day /year) | Discharge date (month/day /year) | %EFPD |
|---|---|---|---|---|---|---|---|
| | | | Pressurized water reactor fuel assemblies | | | | |
| PWR1 | 15x15 AFA3GAA | 4.10 | 52.630 | 4.2 | 5/4/2005 | 5/28/2009 | 89 |
| PWR2 | 15x15 AFA3GAA | 3.93 | 49.555 | 4.2 | 5/4/2005 | 5/29/2009 | 83 |
| PWR3 | 17x17 Fra | 3.69 | 48.175 | 13.1 | 7/6/1996 | 6/21/2000 | 83 |
| PWR4 | 17x17 HTP | 3.93 | 46.873 | 5.2 | 9/26/2004 | 6/4/2008 | 87 |
| PWR5 | 17x17 HTP | 3.94 | 46.866 | 5.2 | 9/26/2004 | 6/2/2008 | 87 |
| PWR6 | 17x17 AA | 3.60 | 45.658 | 14.1 | 7/8/1993 | 6/23/1999 | 52 |
| PWR7 | 17x17 Siemens | 3.94 | 44.483 | 6.1 | 9/5/2003 | 6/27/2007 | 80 |
| PWR8 | 17x17 W | 3.30 | 44.375 | 24.9 | 8/20/1984 | 9/11/1988 | 75 |
| PWR9 | 15x15 W | 3.71 | 45.846 | 6.0 | 6/15/2003 | 8/1/2007 | 76 |
| PWR10 | 17x17 Fra | 3.70 | 43.474 | 15.1 | 7/1/1994 | 6/17/1998 | 75 |
| PWR11 | 17x17 Fra | 3.51 | 43.225 | 13.1 | 7/1/1994 | 6/21/2000 | 50 |
| PWR12 | 17x17 W | 3.30 | 42.969 | 24.9 | 8/20/1984 | 9/11/1988 | 72 |
| PWR13 | 15x15 KWU | 3.20 | 40.920 | 26.3 | 7/25/1982 | 4/25/1987 | 59 |
| PWR14 | 17x17 Fra | 3.51 | 40.745 | 16.1 | 7/8/1993 | 6/24/1997 | 70 |
| PWR15 | 17x17 W | 2.80 | 40.473 | 26.0 | 4/17/1982 | 8/27/1987 | 52 |
| PWR16 | 17x17 Fra | 3.60 | 40.410 | 17.1 | 6/23/1993 | 6/21/1996 | 92 |
| PWR17 | 17x17 Fra | 3.70 | 40.294 | 13.9 | 9/22/1994 | 9/1/1999 | 56 |
| PWR18 | 17x17 Fra | 3.52 | 39.756 | 18.2 | 7/9/1989 | 6/9/1995 | 46 |
| PWR19 | 15x15 KWU | 3.20 | 35.027 | 28.3 | 5/17/1980 | 5/1/1985 | 48 |
| PWR20 | 17x17 W | 3.10 | 34.032 | 27.1 | 7/4/1980 | 6/18/1986 | 39 |
| PWR21 | 17x17 W | 3.10 | 34.019 | 27.1 | 7/4/1980 | 6/18/1986 | 39 |
| PWR22 | 17x17 W | 2.80 | 31.165 | 27.0 | 4/18/1982 | 8/10/1986 | 50 |
| PWR23 | 17x17 Fra | 3.60 | 28.499 | 17.1 | 7/7/1993 | 6/21/1996 | 66 |
| PWR24 | 17x17 W | 2.10 | 23.151 | 18.2 | 7/2/1980 | 6/9/1995 | 11 |
| PWR25 | 17x17 W | 2.10 | 19.607 | 29.2 | 7/3/1980 | 5/24/1984 | 35 |
| | | | Boiling water reactor fuel assemblies | | | | |
| BWR1 | SVEA-96S | 4.01 | 46.41 | 8.3 | 10/28/1999 | 8/29/2006 | 62 |
| BWR2 | SVEA-100 | 3.2 | 43.76 | 10.3 | 6/9/1999 | 8/17/2004 | 77 |
| BWR3 | SVEA-100 | 3.4 | 44.36 | 12.3 | 10/13/1993 | 8/3/2001 | 51 |
| BWR4 | SVEA-100 | 3.4 | 41.89 | 12.3 | 10/28/1999 | 8/29/2006 | 57 |
| BWR5 | SVEA-96S | 3.14 | 42.02 | 8.3 | 10/28/1999 | 8/29/2006 | 56 |
| BWR6 | 8x8 | 2.65 | 38.15 | 29.2 | 10/11/1993 | 8/3/2001 | 48 |
| BWR7 | SVEA-100 | 3.15 | 41.24 | 10.3 | 6/9/1999 | 8/17/2004 | 73 |
| BWR8 | ATRIUM 10B | 3.15 | 39.75 | 9.5 | 8/29/2001 | 5/19/2005 | 97 |
| BWR9 | SVEA-96S | 4.01 | 40.44 | 7.2 | 8/29/2001 | 9/7/2007 | 61 |
| BWR10 | SVEA-96S | 3.14 | 39.50 | 8.3 | 8/29/2001 | 8/29/2006 | 72 |
| BWR11 | 8X8-1 | 2.09 | 31.53 | 22.3 | 9/15/1995 | 7/25/2003 | 45 |
| BWR12 | SVEA-96 | 2.96 | 33.51 | 9.5 | 6/24/1997 | 6/10/2005 | 38 |
| BWR13 | SVEA-96 | 2.96 | 36.83 | 9.5 | 6/24/1997 | 6/10/2005 | 42 |
| BWR14 | 8x8 | 2.65 | 30.49 | 29.2 | 9/3/1987 | 8/12/1992 | 67 |
| BWR15 | 8x8-1 | 2.09 | 29.42 | 25.3 | 8/26/1988 | 5/21/1996 | 42 |
| BWR16 | 8x8-1 | 2.09 | 26.82 | 27.5 | 8/29/1988 | 10/14/1993 | 64 |
| BWR17 | 8x8 | 2.31 | 32.71 | 28.4 | 3/1/1975 | 7/15/1986 | 26 |
| BWR18 | 8x8-1 | 2.09 | 21.52 | 22.3 | 7/23/1994 | 8/30/2000 | 48 |
| BWR19 | 8x8 | 1.27 | 30.80 | 25.5 | 10/17/1984 | 6/10/1989 | 60 |
| BWR20 | SVEA-96 | 2.96 | 26.43 | 9.5 | 8/2/1998 | 6/10/2005 | 35 |
| BWR21 | 8x8 | 2.31 | 27.67 | 27.4 | 3/1/1975 | 7/1/1987 | 20 |
| BWR22 | SVEA-96 | 2.96 | 20.41 | 9.5 | 7/14/2001 | 6/10/2005 | 48 |
| BWR23 | SVEA-96 | 2.96 | 15.99 | 9.5 | 5/24/1999 | 6/10/2005 | 24 |
| BWR24 | 8x8 | 1.27 | 13.32 | 27.4 | 10/17/1984 | 7/10/1987 | 45 |
| BWR25 | 8X8 | 1.27 | 9.13 | 27.4 | 10/17/1984 | 7/10/1987 | 31 |

**Table 1**: Fuel characteristics for the measured PWR and BWR assemblies

## 3. Fork detector design

Measurements were performed with PWR and BWR Fork detector instruments provided by EURATOM. Each arm of these instruments contains a gamma ionization chamber operated in current mode and two neutron fission chambers. One fission chamber is bare to measure primarily thermal neutrons; the other is embedded in a polyethylene region covered by cadmium to measure epithermal and fast neutrons. The gamma detectors are LND model 52110, filled with Xe gas at 10 bars, with a 16 mm diameter and an active length of 86 mm. The neutron fission chambers, CENTRONIC model FC167, contain approximately 160 mg $^{235}$U (93% enriched) and are filled with Ar and N at 4.5 bars; they have a diameter of 25.4 mm and an active length of 127 mm.

The PWR Fork detector assembly used in the measurement is shown in Fig. 1. A cross-sectional view of one detector arm containing the three chambers and their arrangement is shown in Fig. 2. The neutron signals from the two fission chambers of the same kind (bare or cadmium-covered) in each arm of the detector are integrated to compensate for potential radial burnup gradients in the fuel assembly. The signals from the bare fission chambers are registered in Channel A, and the signals from the cadmium-covered chambers are registered in Channel B.


Fig. 1 PWR Fork detector assembly.

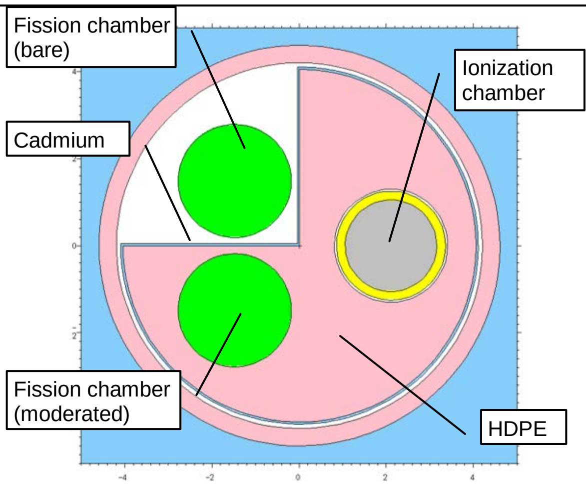


Fig. 2 Cross section of Fork detector arm showing configuration (MCNP detector model).

## 4. Spent fuel data analysis module

The iRAP review and analysis software includes a spent fuel analysis module that performs automated analysis of Fork detector measurements based on operator-declared information on each assembly. This verification approach does not try to estimate enrichment, burnup, or cooling time independently of the operator information; rather, it uses the declared data to predict the neutron and gamma signals, compares the predictions to the measurements and thus identifies potential discrepancies in operator declarations.

The spent fuel analysis module uses the ORIGEN code [7] to perform the burnup and decay calculations. This module can use all information available on the irradiation history of an assembly to calculate the neutron and gamma ray emission rates and energy distribution in the fuel. The ORIGEN calculations use cross-section libraries that have been developed for most classes of fuel assembly designs. For each assembly design, cross-section data are tabulated in libraries as a function of initial enrichment, burnup, and moderator density (for BWR designs). The Fork detector signal is determined by combining the emission rates in the fuel predicted by ORIGEN with energy-dependent detector response functions that have been pre-calculated for the fuel assembly–detector configurations using MCNP. This procedure allows neutron and gamma ray signals to be calculated from assembly declarations in typically less than 5 seconds. The information returned to iRAP by the calculation includes (1) irradiated uranium isotopic contents, (2) plutonium isotopic contents, (3) the gamma ion chamber response, and (4) the neutron fission chamber response for both the bare and cadmium-covered detectors. This system has been described previously [3-5].

A limitation of the spent fuel analysis software identified in previous research [5] is that subcritical neutron multiplication in an assembly was not considered. The methods described above for the neutron response include only the primary emission neutrons without neutron multiplication. The neutron source calculated by ORIGEN includes the delayed neutron emission from spontaneous fission ($^{242}$Cm and $^{244}$Cm are usually dominant) and from ($\alpha$, n) reactions from $^{17}$O, $^{18}$O, and any other light element in the fuel. Subcritical neutron multiplication in the assembly is dependent on the composition of the fuel (the amount of residual fissile material and neutron absorber nuclides); the geometry (leakage); and absorption in water, which may contain soluble boron. Most discharged fuel generally has a similar effective neutron multiplication factor ($k_{\mathrm{eff}}$) and therefore similar induced neutron source multiplication. However, for the fuel assemblies measured at Clab with diverse characteristics, the neutron multiplication varies significantly from one assembly to another. For assemblies that were irradiated beyond typical burnup, neutron multiplication will be reduced, leading to lower neutron counts. For assemblies with low burnup, the higher residual fissile content will increase multiplication and will increase the Fork detector count rate.

A correction for neutron multiplication was added to the spent fuel module for the analysis of the Clab measurements in this work. Neutron multiplication is given approximately as $M = 1/(1 - k_{\mathrm{eff}})$.To avoid time-consuming criticality calculations to determine $k_{\mathrm{eff}}$ for each assembly, neutron multiplication is approximated using the infinite neutron generation factor $k_\infty$ calculated directly by ORIGEN as the neutron production rate divided by the neutron absorption rate in the fuel:

$$k_\infty = \frac{\sum_{i=1} n_i \sigma_{f,i} \bar{\nu}}{\sum_{i=1} n_i \sigma_{abs,i}},$$

where $n$ is the number density of a given nuclide, $\sigma_f$ is the fission cross-section, $\bar{\nu}$ is the average neutrons per fission, and $\sigma_{abs}$ is the total absorption cross-section. The summation is carried over all nuclides in the system. This expression does not consider neutron absorption in assembly structures or water, or leakage. A non-leakage probability factor ($P_{\mathrm{NL}}$) for a single assembly in water is applied, so that $k_{eff} = k_\infty P_{\mathrm{NL}}$, where $P_{\mathrm{NL}}$ is determined for each assembly design class using a detailed neutron transport calculation. A value $P_{\mathrm{NL}} = 0.7$ was applied for analysis of the Clab measurements. This value depends on the soluble boron level in the storage pool. The storage pool at the Clab facility does not contain boron. In pools that contain boron, provided the boron level remains constant at the facility, the effect of boron can be captured in the neutron calibration factor for the instrument.

## 5. Measurement campaigns

Fork detector measurements were performed by EURATOM in two campaigns at Clab. Fifteen of the 25 PWR assemblies (as shown in Table 1) were measured during October 14-15, 2014. The remaining assemblies are scheduled to be measured later in 2015. The 25 BWR assemblies (Table 1) were measured on March 22, 2015. Separate Fork detectors were used for the PWR and BWR measurements due to the different sizes of the assemblies. At the time of the present analysis, detailed operating history data were not available for 10 of the 25 BWR assemblies. Therefore, only results for the 15 BWR assemblies with detailed data are included in the present analysis.

The data acquisition time was approximately 3 minutes per assembly. The relative standard deviation of the measurements was approximately 1% to 3%. Channel A count rate exhibited some erratic behaviour during the BWR measurement campaign, as identified by anomalies in the ratio of the Channel A and B count rates. Consequently, only the results from channel B were used in the analysis presented here. The measurement results for the PWR and BWR assemblies are listed in Table 2. This table shows the calculated neutron and gamma ray signals, both uncorrected and corrected, based on detailed information of the fuel provided by SKB. This detailed information may not always be provided by a reactor operator. The comparisons between measurement (M) and calculation (C) are also included in the table. For the neutron count rates, the correction was made to account for the subcritical neutron multiplication as described in Section 4. For the gamma ray signals, the correction was made to account for the nonlinearity of the ion chamber response (more detailed explanations are included in the next section). Discussions about the comparisons are provided in the next section.

| Assembly | Measured | | Calculated | | | | C/M-1(%) | | | |
|---|---|---|---|---|---|---|---|---|---|---|
| | | | Uncorrected | | Corrected | | Uncorrected | | Corrected | |
| | Neutron (cps) | Gamma (units) | Neutron (cps) | Gamma (units) | Neutron (cps) | Gamma (units) | Neutron | Gamma | Neutron | Gamma |
| Pressurized water reactor fuel assemblies | | | | | | | | | | |
| PWR1 | 2162.1 | 1223182 | 2321.1 | 1441610 | 2263.1 | 1253397 | 7.4 | 17.9 | 4.7 | 2.5 |
| PWR2 | 1837.9 | 1126913 | 1795.3 | 1259584 | 1828.6 | 1125102 | -2.3 | 11.8 | -0.5 | -0.2 |
| PWR3 | 1246.4 | 612000 | 1312.1 | 588625 | 1216.1 | 612183 | 5.3 | -3.8 | -2.4 | 0.0 |
| PWR4 | 1522.0 | 934477 | 1404.3 | 1020117 | 1468.0 | 950452 | -7.7 | 9.2 | -3.6 | 1.7 |
| PWR6 | 1049.3 | 562908 | 1105.8 | 525230 | 1034.0 | 558843 | 5.4 | -6.7 | -1.5 | -0.7 |
| PWR7 | 1169.3 | 802432 | 1091.0 | 852702 | 1167.6 | 823471 | -6.7 | 6.3 | -0.1 | 2.6 |
| PWR9 | 1395.5 | 859405 | 1408.2 | 890628 | 1432.4 | 852644 | 0.9 | 3.6 | 2.6 | -0.8 |
| PWR10 | 798.5 | 531171 | 798.2 | 488502 | 785.7 | 527356 | 0.0 | -8.0 | -1.6 | -0.7 |
| PWR11 | 817.4 | 517900 | 829.8 | 489221 | 818.8 | 527976 | 1.5 | -5.5 | 0.2 | 1.9 |
| PWR14 | 666.2 | 486164 | 622.0 | 439165 | 625.8 | 484298 | -6.6 | -9.7 | -6.1 | -0.4 |
| PWR16 | 590.0 | 480941 | 570.5 | 420549 | 577.0 | 467804 | -3.3 | -12.6 | -2.2 | -2.7 |
| PWR19 | 245.8 | 338518 | 258.2 | 257907 | 256.5 | 316360 | 5.0 | -23.8 | 4.3 | -6.5 |
| PWR22 | 205.5 | 319391 | 209.9 | 243437 | 209.3 | 302078 | 2.1 | -23.8 | 1.9 | -5.4 |
| PWR23 | 163.1 | 359146 | 130.3 | 298237 | 165.8 | 355353 | -20.1 | -17.0 | 1.7 | -1.1 |
| PWR24 | 149.9 | 263198 | 162.2 | 202231 | 170.0 | 260428 | 8.2 | -23.2 | 13.4 | -1.1 |
| Boiling water reactor fuel assemblies | | | | | | | | | | |
| BWR1 | 1034.7 | 501985 | 1140.3 | 567202 | 1050.4 | 531017 | 10.2 | 13.0 | 1.5 | 5.8 |
| BWR2 | 843.2 | 477075 | 883.5 | 506707 | 839.4 | 485204 | 4.8 | 6.2 | -0.4 | 1.7 |
| BWR5 | 738.4 | 494300 | 768.2 | 518009 | 750.1 | 493842 | 4.0 | 4.8 | 1.6 | -0.1 |
| BWR7 | 756.7 | 451088 | 744.3 | 475366 | 731.9 | 461043 | -1.6 | 5.4 | -3.3 | 2.2 |
| BWR8 | 679.0 | 463648 | 646.7 | 498980 | 658.4 | 479275 | -4.8 | 7.6 | -3.0 | 3.4 |
| BWR9 | 641.0 | 520513 | 664.8 | 549400 | 675.2 | 517642 | 3.7 | 5.5 | 5.3 | -0.6 |
| BWR10 | 629.8 | 505537 | 617.8 | 519270 | 635.1 | 494804 | -1.9 | 2.7 | 0.8 | -2.1 |
| BWR12 | 375.0 | 397132 | 343.4 | 377655 | 374.5 | 383526 | -8.4 | -4.9 | -0.1 | -3.4 |
| BWR13 | 525.3 | 427656 | 490.5 | 415504 | 503.3 | 413979 | -6.6 | -2.8 | -4.2 | -3.2 |
| BWR19 | 193.3 | 234132 | 182.5 | 215353 | 180.3 | 244702 | -5.6 | -8.0 | -6.7 | 4.5 |
| BWR20 | 164.8 | 341681 | 134.9 | 308797 | 175.3 | 326480 | -18.1 | -9.6 | 6.4 | -4.4 |
| BWR22 | 52.9 | 268423 | 32.6 | 223775 | 57.7 | 252329 | -38.3 | -16.6 | 9.0 | -6.0 |
| BWR23 | 23.6 | 220091 | 9.6 | 169824 | 22.7 | 202357 | -59.5 | -22.8 | -3.9 | -8.1 |
| BWR24 | 21.4 | 109311 | 21.8 | 88574 | 24.6 | 120216 | 2.0 | -19.0 | 14.9 | 10.0 |
| BWR25 | 7.1 | 81625 | 5.1 | 59782 | 7.1 | 87776 | -28.4 | -26.8 | 0.7 | 7.5 |

**Table 2:** Comparison of measured neutron (channel B) and gamma detector signals with calculations. Neutron calculations are shown with and without correction for subcritical multiplication. Gamma calculations are shown with and without correction for nonlinearity of the ion chamber response

# 6. Analysis

## 6.1 Gamma signals

An initial review of the gamma data (uncorrected) in Table 2 showed significant deviations of up to +18% and -27% compared to measured signals. The discrepancies exhibit clear trends with the gamma signal intensity, indicating a nonlinear detector response. This behaviour does not exhibit saturation at high gamma ray intensities, but rather, exhibits a strong power relationship over the range of the predicted signals.

Detector response of the LND model 52110 gamma ion chambers used in the measurements has previously been measured using a calibrated Keithly ionization chamber and a $^{60}$Co source in water. Nonlinear behaviour is also evident in the calibrated response data, yielding a well-defined power relationship of $y = x^p$, where $p$ = 0.575 with an $R^2$ fit coefficient of 0.9995 over more than 5 orders of magnitude of gamma ray dose rate.

The gamma ion chamber response for both the PWR and BWR measurement campaigns at Clab also indicates a nonlinear power relationship, as was observed in the $^{60}$Co calibration data. However, a power coefficient of $p$ = 0.8 with an $R^2$ value of 0.996 was found over the range of the Clab data, representing a factor of more than 30 in ion chamber response. The cause of the differences in ion chamber response may be due to the detectors, electronics, sources, or detector performance in a mixed neutron and gamma environment. Assuming a power relationship for the gamma detector response, the predicted gamma ray signals were corrected for the nonlinear behaviour. The results, shown in Table 2 as corrected gamma data, show that the discrepancies observed before correction are largely eliminated and that most results are within ± 5%. The gamma results, plotted in Fig. 3, show the predicted gamma signal as a function of the measured signal before and after correction. The BWR assemblies have lower signals, caused primarily by the smaller assembly size and lower quantities of actinides and fission products.

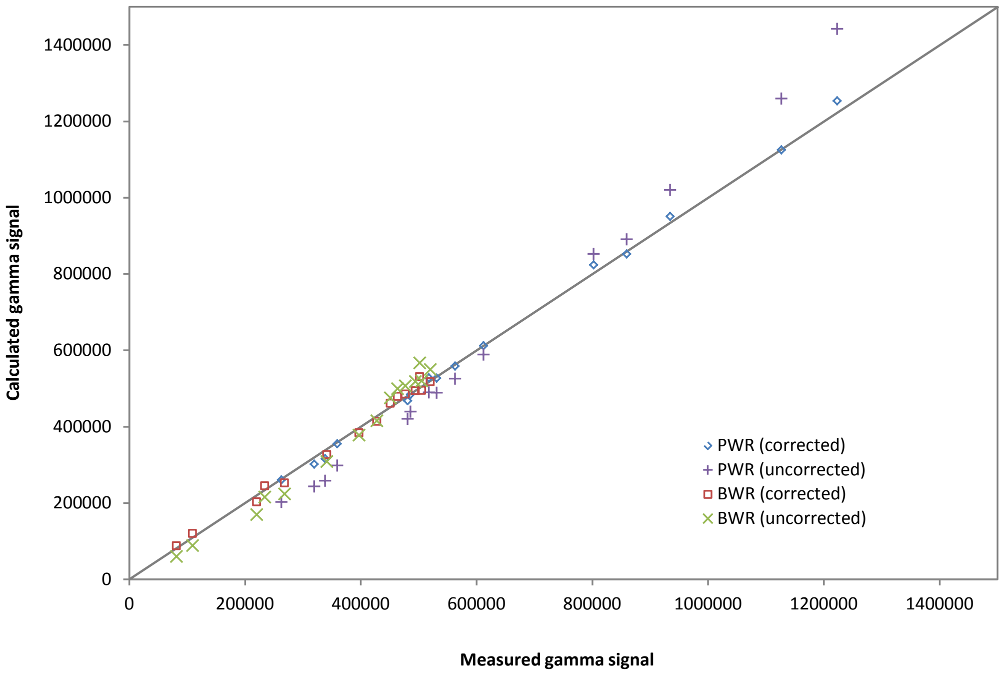


Fig. 3. Comparison of measured and calculated (uncorrected and corrected for ion chamber response) gamma ion chamber signals for PWR and BWR assemblies.

### 6.2 Neutron count rates

The measured and calculated neutron count rates in Table 2 are illustrated in Fig. 4. Results with and without the correction for subcritical neutron multiplication are given. Good agreement is generally observed between calculations (corrected) and measurements for most assemblies, with only one PWR and one BWR assembly exhibiting a difference greater than 10%. The range of neutron data spans more than a factor of 100 in fission chamber response. The largest deviations are observed for both the lowest burnup PWR and BWR assemblies. Assembly BWR #24 had a count rate of 21 cps compared to more than 1000 cps for BWR #1, and also had a very low burnup of 13 GWd/tU and an enrichment of only 1.27 wt% $^{235}$U.

The impact of the neutron multiplication correction for the SKB assembly analysis is seen to be significant. Excluding the correction resulted in larger deviations for almost all assemblies. For example, assembly PWR #23 experienced a burnup that was less than most assemblies with similar enrichments, resulting in relatively more residual fissile material in the assembly that increases neutron multiplication. Including the neutron multiplication correction decreased the discrepancy with measurements from 20% to less than 2%. The effect of the multiplication correction was not as evident in previously evaluated loading campaign data due to the similarity of many of the assemblies.

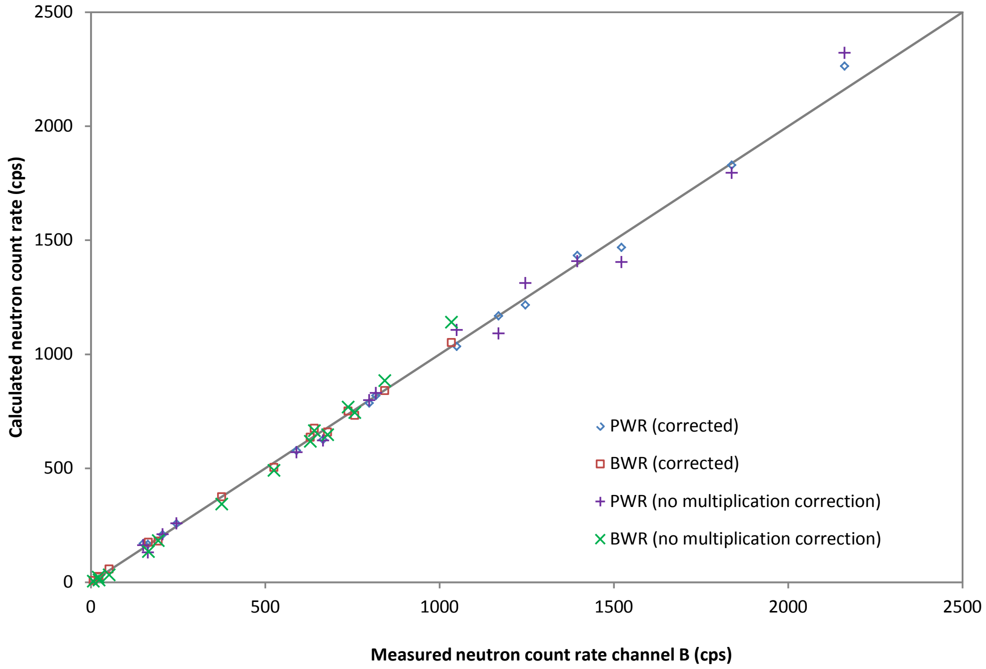


Fig. 4. Comparison of measured and calculated (uncorrected and corrected for subcritical neutron multiplication) neutron fission chamber count rates for PWR and BWR assemblies.

The relative standard deviation of the percent differences between calculated (after correction) and measured gamma signals, shown in Table 2 and plotted in Fig. 5, is 2.4% for the 15 PWR assemblies and 5.2% for the 15 BWR assemblies. The largest deviations occur for the BWR assemblies #23, #24, and #25. These assemblies experienced very low burnup and had the lowest gamma signals of all measured assemblies. Using a 95/95 two-sided tolerance interval and 15 measurements, and assuming a normal distribution, 95% of measured PWR assemblies are expected in an interval of ± 7% of the predicted values based on declarations with a 95% probability. For the BWR measurements, the 95% tolerance interval is ± 15%.

The relative standard deviation of the percent differences between calculated and measured neutron signals (Fig. 5) is 4.6% for the 15 PWR assemblies and 5.7% for the 15 BWR assemblies. Similar to the gamma results, the largest deviations occur for the low-burnup assemblies that had the smallest neutron signals. Using a 95/95 two-sided tolerance interval and 15 measurements, a 95% tolerance range of ± 14% is expected for the PWR measurements. For the BWR measurements, the 95% tolerance interval is ± 17%. All assemblies measured at SKB are within these tolerance ranges.

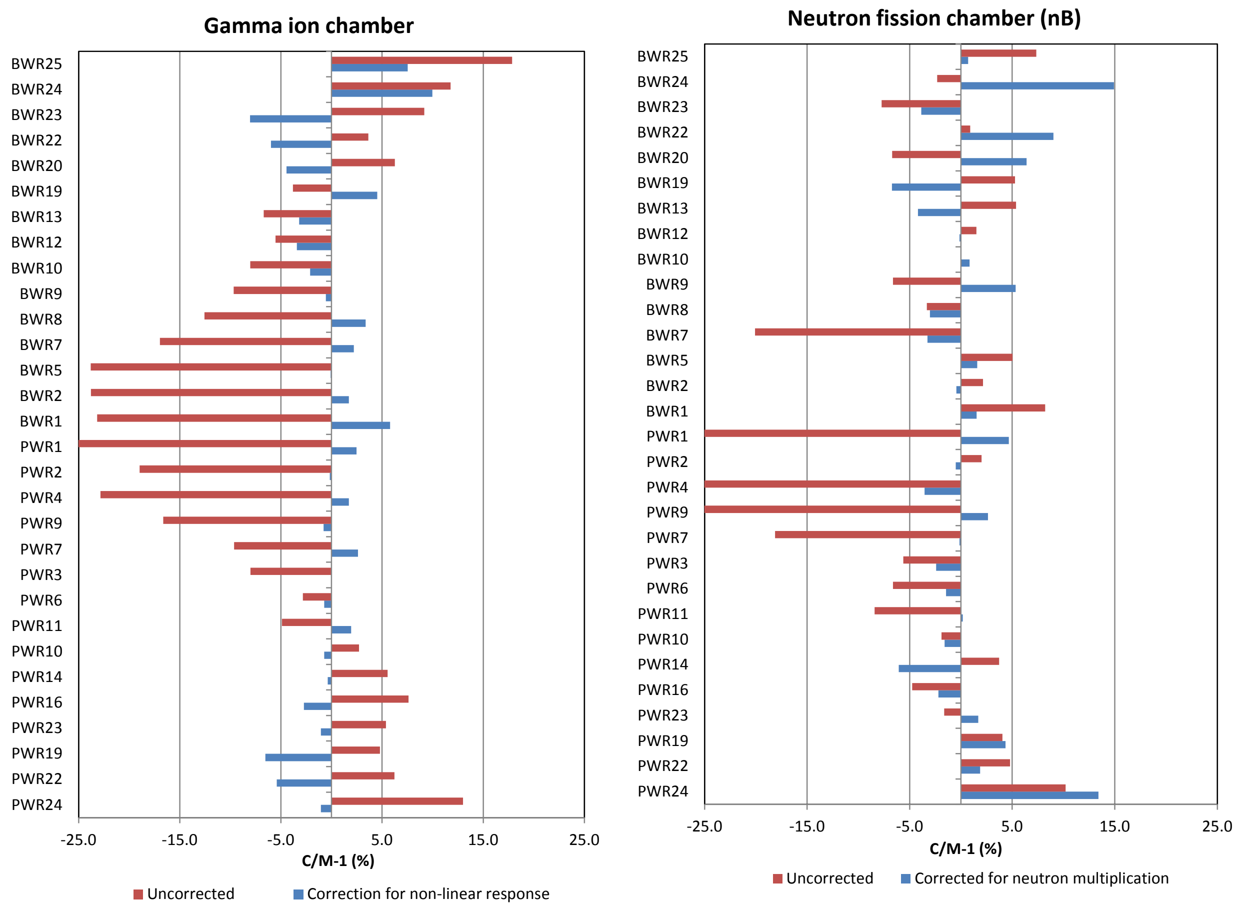


Fig. 5. Percent deviation between calculated and measured gamma ion chamber results (left) and neutron fission chamber (Channel B) results (right) for the SKB assemblies.

## 7. Uncertainties

Uncertainties are attributed to the measurements (counting and assembly positioning uncertainties), the declarations, and the analysis. These uncertainties define the ability to identify discrepancies in declarations and verify the integrity of the nuclear material. The main contributors to uncertainty in the spent fuel analysis method are described in this section.

### 7.1 Accuracy of the records

The assembly burnup declaration is obtained from reactor simulation codes and is generally accurate to 2% to 3% [8]. For typically discharged fuel, this burnup uncertainty results in an uncertainty in the gamma signal of similar magnitude (2% to 3%) and an uncertainty in the activity of the major neutron-emitting actinides of up to 6% for $^{242}$Cm and 13% for $^{244}$Cm. Therefore, achieving accuracy in the neutron count rate verification of less than ~10% will be limited by the uncertainty in the reactor records.

### 7.2 Operating history

Information on the operational details of an assembly may not be available to the inspector, including dates when the assembly resided in the reactor and the accumulated burnup by operating cycles that can be used (if available) to derive the specific power of the assembly during its irradiation history. Information on non-continuous assembly irradiation in the reactor (if removed for some cycles and then re-loaded in the core) can have a significant effect on both neutron and gamma signals due to the half-lives of the dominant nuclides: $^{154}$Eu (8.6 yrs), $^{134}$Cs (2.07 yrs), $^{137}$Cs (30 yrs), $^{242}$Cm (163 days), and $^{244}$Cm (18.1 yrs). Other operational variables include the exposure to control absorbers, discrete burnable absorber rods, or control blades.

Detailed operating histories for the assemblies measured at Clab were provided by SKB and they were used in this analysis. To further quantify the uncertainties introduced by the lack of detailed data, additional analysis using only standard safeguards data (e.g., just fuel burnup without cycle history information) on these measurements are being performed and the results will be reported in the future.

### 7.3 Fuel and assembly design

Assembly designs are modelled using representative design information that approximates the range of design variations in use, and these approximations contribute to uncertainty. Although the class of assembly design(s) in a facility is usually known, other variables, such as presence of integral burnable absorber rods (e.g., gadolinium) and enrichment zoning (variation of rod enrichments in the assembly), are typically unknown to the inspector.

### 7.4 Axial burnup distribution

The assembly average burnup is reported by the operator; however, Fork detector measurements are typically performed at the mid-section of the assembly. The assembly burnup is adjusted in this analysis using a factor of 1.06 for PWR assemblies and 1.16 for BWR assemblies. This factor is estimated as the ratio of assembly centreline burnup to the assembly average burnup.. An analysis using the actual centreline burnup of each measured SKB assembly indicates that the variability in the axial burnup profile introduces an uncertainty of less than 1.5% in the centreline burnup, with variations of up to 5% observed for several low-burnup assemblies that have larger axial peaking factors.

### 7.5 Repeatability of the measurements

Uncertainty attributed to positioning of the assembly in the Fork detector was evaluated and the variability was found to be generally less than 1% in the gamma signal. The neutron channel B results showed differences of 1% to 2% and the neutron channel A showed differences of 3% to 5% when the same assembly was measured multiple times. The larger sensitivity observed in channel A may be due to the fact that the bare neutron fission chambers measure primarily thermal neutrons that are sensitive to any changes in moderation.

### 7.6 Assembly rotational uncertainty

The two Fork arms, each containing separate detectors, are designed to compensate for potential burnup gradients in the assembly that may lead to non-uniform neutron and gamma emission rates. The Fork measurements were repeated on three PWR assemblies with small and large radial burnup gradients after the assemblies were rotated in 90° steps. The gamma signal was found to have a small dependency on rotation (~1% variation). The neutron channel B also exhibited low dependence (about 1% to 2%); the neutron channel A had the largest dependence (about 2% to 4%).

### 7.7 Nonlinear gamma detector response

Corrections to the LND gamma ion chamber signals were required to compensate for apparent nonlinear response. The correction factor between the minimum and maximum gamma signal was larger than 40% over the range of the PWR assemblies. The gamma response was different from responses observed in earlier LND detector calibration measurements performed using a $^{60}Co$ source. It has not yet been determined whether the response is associated with the source energy spectrum, the ion chamber design, detector performance in mixed gamma and neutron fields, the detector operating regime, and/or the associated electronics. Linear response behaviour, or the ability to reliably correct for nonlinear response, will be a critical requirement to apply the Fork detector for quantitative spent fuel verification applications.

## 8. Conclusions

Safeguards agencies are facing increasing near-term spent fuel verification challenges from the expanding use of dry cask storage and with the planned repositories in Sweden and Finland.

EURATOM has identified data quality (better instruments and improved data evaluation to reduce false alarms) and resources (better efficiency and reduced costs) as key near-term support needs.

The research described in this paper addresses both improved data evaluation efficiency and improved accuracy by using rigorous modelling and simulation software and nuclear data. The analysis methods implemented in iRAP have been upgraded based on initial instrument testing and applied to measure a very diverse set of assemblies at the SKB Clab facility. These developments enable advancement of the Fork detector from a qualitative measurement instrument used frequently as an attribute test, or with limited semi-empirical analysis, to a fully quantitative instrument capable of verifying operator declarations with improved accuracy.

This research also points to a need for instrument improvements. The ion chamber response was found to be nonlinear with the gamma ray signal, which represents a potential roadblock for wider quantitative application of the Fork detector. Alternative gamma instruments, such as the Cadmium-Zinc-Telluride (CdZnTe) detector, that have been previously investigated for application to the Fork [9, 10] may provide a practical and cost-effective near-term solution.

Finally, while verification of operator declarations of spent fuel is one of the goals of the IAEA, safeguards inspections must also verify the integrity of a fuel assembly to determine that nuclear contents have not been diverted from intended use. Quantitative application of the Fork detector will enable improved partial defect detection by identifying statistically significant discrepancies between the predicted and measured signals. The level of partial defect detection (fraction of fuel being removed from the assembly) will be dependent on the detector performance, as is quantified in this paper. With improved quantitative analysis and review of the measurement data, the ability to detect partial defects is likely to be significantly better than the current 50% partial defect level, as is frequently cited for the Fork detector.

## 9. Acknowledgements

This work has been funded by the International Nuclear Safeguards Engagement Program (INSEP) under the Office of Nonproliferation and Arms Control of the National Nuclear Security Administration, U.S. Department of Energy, and by the European Commission. The Fork measurements performed at the Clab facility in Sweden were made possible with the support of the Swedish Nuclear Fuel and Waste Management Company, SKB.

## 10. References

1. A. Lebrun, S. Jung, S. Zykov, and A. Berlizov; *Status of NDA Techniques in Use for the IAEA Verification of Light Water Reactor Spent Fuel*; INMM (ISBN: 978-1-62993-580-5); 2013.
2. Schwalbach, P., et al.; *RADAR: EURATOM's Standard for Unattended Data Acquisition*; Proc. Int. Atomic Energy Agency Symposium Int. Safeguards, Wien, Austria; 2001.
3. Gauld, I. C., et al.; *Applications of ORIGEN to Spent Fuel Safeguards and Non-Proliferation*; Proc. of INMM 47th Annual Meeting, Nashville, Tennessee, 2006.
4. Vaccaro, S., et al.; *Enhanced Spent Fuel Verification by Analysis of Fork Measurements Data Based on Nuclear Modelling and Simulation*; INMM Information Analysis Technologies, Techniques and Methods for Safeguards, Nonproliferation and Arms Control Verification Conference, Portland; May 12–14, 2014.
5. Vaccaro, S., et al.; *A New Approach to Fork Measurements Data Analysis by RADAR-CRISP and ORIGEN Integration*; *Trans. Nucl. Sci*. **61**(4); 2014; p 2161.
6. Tobin, S. J., et al.; *Experimental and Analytical Plans for the Non-destructive Assay System of the Swedish Encapsulation and Repository Facilities*; IAEA Safeguards Symposium 2014, Vienna, Austria; 2014.
7. Gauld, I. C., et al.; *Isotopic Depletion and Decay Methods and Analysis Capabilities in SCALE*; *Nuclear Technology* **174**, 2; 2011; p 169.
8. Electric Power Research Institute; *Determination of the Accuracy of Utility Spent Fuel Burnup Records—Final Report*; EPRI TR-112054; July 1999.
9. Tiitta, A., et al.; *Investigation on the Possibility to Use Fork Detector for Partial Defect Verification of Spent LWR Fuel Assemblies*; STUK-YTO-TR 191; 2002.
10. Doering T. W., and Cordes, G.A.; *Status of the Multi-Detector Analysis System (MDAS) and the Fork Detector Research Programs*; IAEA-TECDOC-1241; 2000; p. 286.